Copy 276
RM L54E19

NACA RM L54E19

NACA

RESEARCH MEMORANDUM

SOME INTERNAL-FLOW CHARACTERISTICS AT ZERO FLIGHT SPEED OF AN ANNULAR SUPERSONIC INLET AND AN OPEN-NOSE INLET WITH SHARP AND ROUNDED LIPS

By Joseph R. Milillo

Langley Aeronautical Laboratory
Langley Field, Va.

NATIONAL ADVISORY COMMITTEE
FOR AERONAUTICS

WASHINGTON

July 6, 1954

NATIONAL ADVISORY COMMITTEE FOR AERONAUTICS

RESEARCH MEMORANDUM

SOME INTERNAL-FLOW CHARACTERISTICS AT ZERO FLIGHT SPEED OF AN ANNULAR SUPERSONIC INLET AND AN OPEN-NOSE INLET WITH SHARP AND ROUNDED LIPS

By Joseph R. Mililo

SUMMARY

Static tests of an annular conical-shock inlet and an open-nose conical inlet with three lip shapes were conducted at the Langley 8-foot transonic tunnel. Measurements of pressure recovery, surface pressure, and total pressure were made through a mass-flow range extending to choking. The results indicate that the two inlets with thin sharp lips had about the same relatively poor pressure-recovery characteristics and choked at a mass-flow rate of about 78 percent of the theoretical maximum. However, both the pressure recovery and choking mass-flow rate were greatly improved by replacing the sharp lip by two alternate shapes with lip roundness and internal contraction just behind the inlet lip.

It was also shown that inlets with thin sharp lips but widely different diffusers and inlet configuration had very similar pressure-recovery characteristics which were adequately defined by theory.

INTRODUCTION

The optimum performance of a turbojet-engine—fixed-area inlet combination at supersonic speeds is obtained when the air flow through the engine-inlet combination is near the maximum permitted by the inlet. At the take-off or low-speed flight condition, the inlet will tend to be operated at a choked or extremely high mass-flow condition and the engine may suffer severe thrust penalties due to losses in total pressure and reductions in effective inlet entrance area. In the case of sharp-lip inlet design, the reduction in engine performance can be quite large at the static or take-off condition.

Some attention has therefore been given to the problem of the performance of such sharp-lip inlets under the aforementioned conditions

(refs. 1 to 3). Tests of round-lip inlets have also been made (ref. 4). In addition to this work, the internal-flow performance of two supersonic-type inlets of the Langley 8-foot transonic tunnel inlet research program were studied under static conditions and the results are presented herein.

The inlets tested were a conical-shock inlet and a nose inlet with three lip shapes - a sharp lip, a round lip, and a bell-type lip. Pressure recovery, lip pressure distribution, total-pressure surveys, and mass-flow measurements are presented for the nose inlet, whereas pressure recovery and mass-flow measurements only are presented for the conical-shock inlet. Mass-flow ratio was varied from about 0.33 to the choking value.

SYMBOLS

A	duct cross-sectional area
D	maximum external diameter (8.0 in., station 2)
H	total pressure (distinguished from pitot pressure)
$\bar{H}$	average total pressure, $\int H \frac{dA}{A}$
m	mass-flow rate
m/m_s	mass-flow ratio, ratio of mass flow through the duct to the mass flow under isentropic conditions through an area equal to inlet minimum area at a Mach number of 1.0, $\frac{\rho V A}{\rho_s V_s A_1}$
p	static pressure
P_a	atmospheric pressure
r	radius
R	body maximum radius, $D/2$
x	axial distance, positive downstream
y	distance from diffuser wall
ϕ	equivalent conical angle of diffuser

Subscripts:

1 minimum-area station at, or just inside, inlet lip (see fig. 1)

2 diffuser exit station (see fig. 1)

3 venturi station (see fig. 1)

APPARATUS AND METHODS

Test equipment.- Figure 1 presents a schematic drawing of the test apparatus. The inlets were mounted on a long tube or barrel that contained the diffuser exit rakes (station 2) and a venturi which contained a rake for the measurement of mass flow and pressure recovery. The low-pressure source was a 10,000 cu ft/min compressor.

Models.- The annular conical-shock inlet was designed to provide enough air for an engine of about 10,000 pounds static thrust at a Mach number of 2.0. The inlet was of wood and plastic construction with a steel leading edge. Dimensions of the inlet are shown in figure 2.

The nose inlet was designed with three interchangeable lip shapes. The shape of the external contour of the inlet remained the same as did the minimum area and equivalent conical angle of the diffuser. The two parameters that varied were lip shape and length of the inlet preceding the diffuser entrance. The sharp lip of the nose inlet was machined from 24ST aluminum alloy. The bell and round lips and fixed part of the inlet were made of wood, Fiberglas, and Paraplex plastic. A photograph of the nose inlet and lip sections is presented as figure 3(a). Drawings and dimensions of the nose inlet are presented in figures 3(b) and 3(c). The duct-area variation of the conical-shock inlet and the nose inlet are presented in figure 4.

Test procedure.- For each inlet the back pressure was reduced through several intermediate steps until the inlet was choked. The back pressure was then further reduced to increase the inlet losses and define adequately the choking mass-flow ratio. Pressure readings were recorded simultaneously by photographing a multitube manometer.

Data were recorded by a survey rake located at a forward survey station during several tests with the nose inlet (see fig. 3(b)). Total-pressure-recovery data obtained from the other rakes during these tests are not presented.

Methods and accuracy.- The mass-flow ratio and pressure recovery were obtained by numerical integration of the venturi-rake data. Because of very low Mach numbers between station 2 and the entrance to the venturi, the total-pressure losses were relatively small between the two stations. The indicated pressure recovery at the diffuser exit (station 2) was about 0.01 higher than the pressure recovery presented herein throughout the mass-flow range.

The accuracy of measurements is estimated as follows:

Mass-flow ratio	$\begin{cases} +0.02 \\ -0 \end{cases}$
Pressure recovery	±0.01
Static and total pressure ratios	±0.01

The accuracy estimate for mass-flow ratio accounts for the combined effects of a ±0.01 random error and a systematic error of 0.01 which resulted from leakage.

RESULTS AND DISCUSSION

Pressure distributions.- Pressure distributions about the inner and outer surfaces of the nose inlet lips are presented in figure 5. For all lip shapes the static pressure increased very rapidly to approximately atmospheric pressure on the outer surface (within 0.50 in. from the leading edge), thereby indicating very low flow velocities over the external surface and consequently little effect of external geometry as was also concluded in reference 4. Just inside the inlet lips, the pressure ratios indicated that local speeds reached values on the order of 1.8 Mach number. Large variations in local Mach number were present along the constant-area duct section of the inlets at the higher mass-flow ratios, especially for the sharp-lip inlet (see fig. 5(a)).

Total-pressure surveys.- Total-pressure surveys at the forward survey station presented in figure 6 indicate the presence of thick boundary layers for all three lip shapes. Application of the separation criterion of reference 5 shows that the boundary-layer profiles are of the unseparated type for the highest mass-flow ratios, but at the lower mass-flow ratios, the calculated boundary-layer-shape factors fall within the range where separation may exist. Total-pressure losses extended entirely across the duct at the highest test mass-flow ratios (inlet-choked condition) and, except for the region immediately adjacent to the duct wall, the flow was supersonic at the forward survey station.

The profiles of the sharp- and round-lip inlets show a region of depressed total pressure in the center of the duct at the highest mass-flow ratios. For both of these inlets, this core of reduced total

pressure is presumed caused by the nature of a shock pattern existent near the duct entrance. Figure 7 presents an estimate of the flow pattern in the sharp-lip inlet, and was drawn from reference to figures 5 and 6 and to the pressure surveys and visual-flow studies of reference 6. Except for the boundary layer and a region downstream from the normal shock in the center of the duct, the flow was supersonic everywhere between the sonic line and some point downstream from the forward survey station. The core of reduced total-pressure air observed at the survey station thus appears to have resulted from the greater losses of the normal shock in the duct center. The supersonic flow through the inclined shock cannot have lost at the shock itself the amount of total-pressure loss indicated by the level of the total-pressure-ratio curve between $y/r = 0.3$ and $y/r = 0.6$ in figure 6. Additional total-pressure losses accrued to this flow through mixing with the boundary layer and the subsonic flow region behind the normal shock. A strong shock is assumed to have terminated the supersonic flow at some point in the diffuser.

Diffuser-exit surveys presented in figure 8 indicate uniform total-pressure distributions about the annulus at low mass-flow ratios but, as choking was approached, large nonuniformities appeared in the flow. The nonuniformities were more pronounced for the round and bell lips than for the sharp lip. For the choked mass-flow ratio corresponding to the lowest test back pressure, the total-pressure distributions for all inlets were more uniform than just prior to choking.

Pressure-Recovery Characteristics

The pressure-recovery characteristics of the inlets are presented in figure 9 as a function of mass-flow ratio. The performance of the two sharp-lipped inlets was quite similar and inferior to that of the other two inlets with the modified lips. By rounding the lip of the nose inlet, both the pressure recovery and choking value of mass-flow ratio were substantially increased. The bell lip resulted in further improvement, increasing the pressure recovery throughout the mass-flow-ratio range and raising the choking mass-flow ratio by more than 20 percent above that of the sharp-lip inlets. The low value of choking mass-flow ratio of the sharp-lip inlet was due to the separation bubble (fig. 7) which reduced the effective minimum area and to the existence of supersonic flow at the effective minimum. The round and bell leading edges tended to alleviate the former condition and resulted in a much higher value of choking mass-flow ratio.

Pressure Recovery of Sharp-Lip Inlets

Available data concerning the pressure-recovery characteristics of sharp-lip inlets at static conditions are presented in figure 10. A

theoretical curve from reference 7 for the sharp-lip inlet at static conditions is also presented in the figure. Although the inlets vary widely in configuration and in diffuser type, rate, and area ratio, the pressure-recovery curves are very similar and agree well with the theory. The theoretical curve accounts for a total-pressure loss at the inlet and a small subsonic diffuser loss. The losses at the inlet were obtained utilizing the momentum balance between the free stream and inlet stations. Inasmuch as the only variable in common among the inlets was a thin sharp lip, the similarity of the curves indicates that total-pressure characteristics at static conditions are mainly determined by details of the lip shape as was also concluded in reference 4. The differences in pressure recovery that exist are probably due to differences in diffuser geometry.

CONCLUSIONS

Tests of an annular supersonic inlet and an open-nose inlet with sharp and rounded lips at static conditions led to the following conclusions:

(1) The two inlets with thin sharp lips had about the same relatively poor pressure recovery characteristics and choked at a mass-flow rate of about 78 percent of the theoretical maximum.

(2) The pressure recovery and choking mass-flow ratio were greatly improved by replacing the sharp lip by two alternate shapes with lip roundness or internal contraction just behind the leading edge.

(3) Inlets with thin sharp lips but widely different configurations had very similar pressure recovery characteristics which were adequately defined by theory.

Langley Aeronautical Laboratory,
National Advisory Committee for Aeronautics,
Langley Field, Va., May 10, 1954.

REFERENCES

1. Scherrer, Richard, Stroud, John F., and Swift, John T.: Preliminary Investigation of a Variable-Area Auxiliary Air-Intake System at Mach Numbers from 0 to 1.3. NACA RM A53A13, 1953.

2. Cortright, Edgar M., Jr.: Preliminary Investigation of a Translating Cowl Technique for Improving Take-Off Performance of a Sharp-Lip Supersonic Diffuser. NACA RM E51I24, 1951.

3. Mossman, Emmet A., and Anderson, Warren E.: The Effect of Lip Shape on a Nose-Inlet Installation at Mach Numbers From 0 to 1.5 and a Method for Optimizing Engine-Inlet Combinations. NACA RM A54B08, 1954.

4. Bryan, Carroll R., and Fleming, Frank F.: Some Internal-Flow Measurements of Several Axisymmetric NACA 1-Series Nose Air Inlets at Zero Flight Speed. NACA RM L54E19a, 1954.

5. Von Doenhoff, Albert E., and Tetervin, Neal: Determination of General Relations for the Behavior of Turbulent Boundary Layers. NACA Rep. 772, 1943. (Supersedes NACA WR L-382.)

6. Blackaby, James R., and Watson, Earl C.: An Experimental Investigation at Low Speeds of the Effects of Lip Shape on the Drag and Pressure Recovery of a Nose Inlet in a Body of Revolution. NACA TN 3170, 1954.

7. Fradenburgh, Evan A., and Wyatt, DeMarquis D.: Theoretical Performance Characteristics of Sharp-Lip Inlets at Subsonic Speeds. NACA TN 3004, 1953.

[redacted]

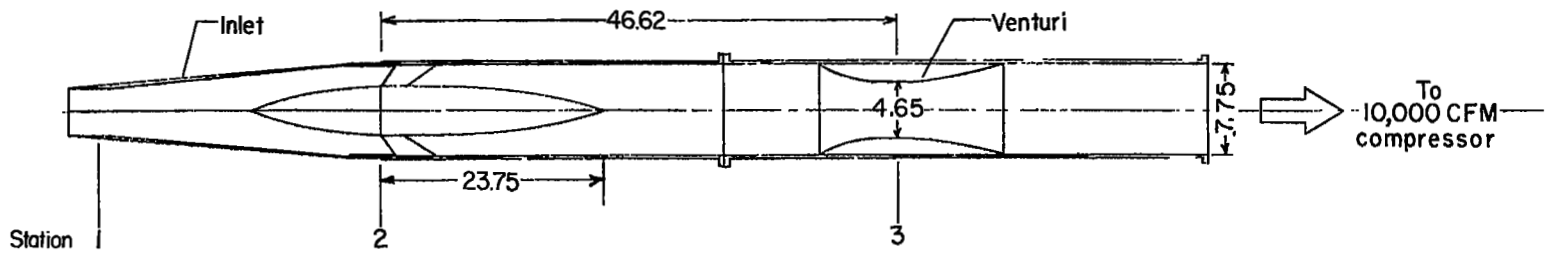

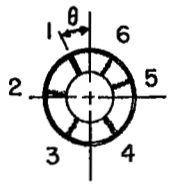

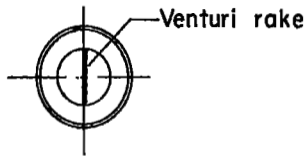

Diffuser rake position

Rake	θ, deg
1	24
2	84
3	134
4	204
5	265
6	315

Figure 1.- Details of static test setup. All dimensions are in inches.

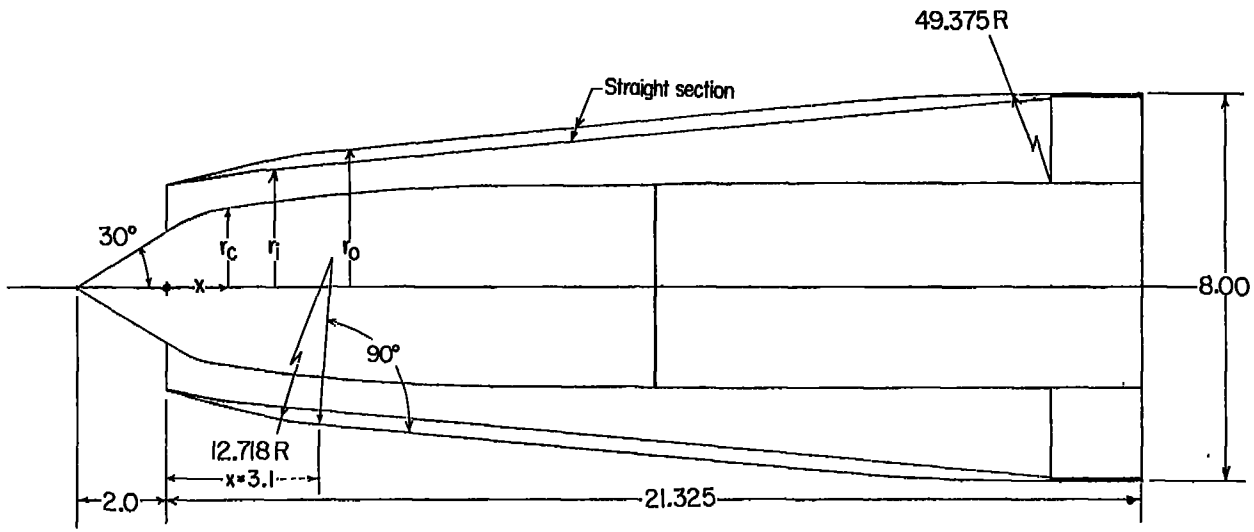

x, in.	r_i, in.	r_o, in.
0	2.116*	2.116**
.125	2.146	2.151
.3125	2.191*	2.203**
.500	2.234	2.250
.6875	2.269	2.295
.875	2.299	2.325
1.0625	2.324	
1.25	2.344♀	
3.625	2.532♀	
19.325	3.815♀	

* 13-1/2° slope between points
** 15-1/2° slope between points
♀ straight line between points
A_{min} = 0.0617 sq ft

x, in.	r_c, in.
-2.00	0
-4.38	1.408
.500	1.445
.600	1.485
.800	1.543
1.00	1.576
1.200	1.604
2.00	1.710
3.00	1.815
5.00	2.015
7.00	2.094
13.00	2.094
22.00	2.156

Figure 2.- Conical-shock inlet and coordinates. All dimensions are in inches.

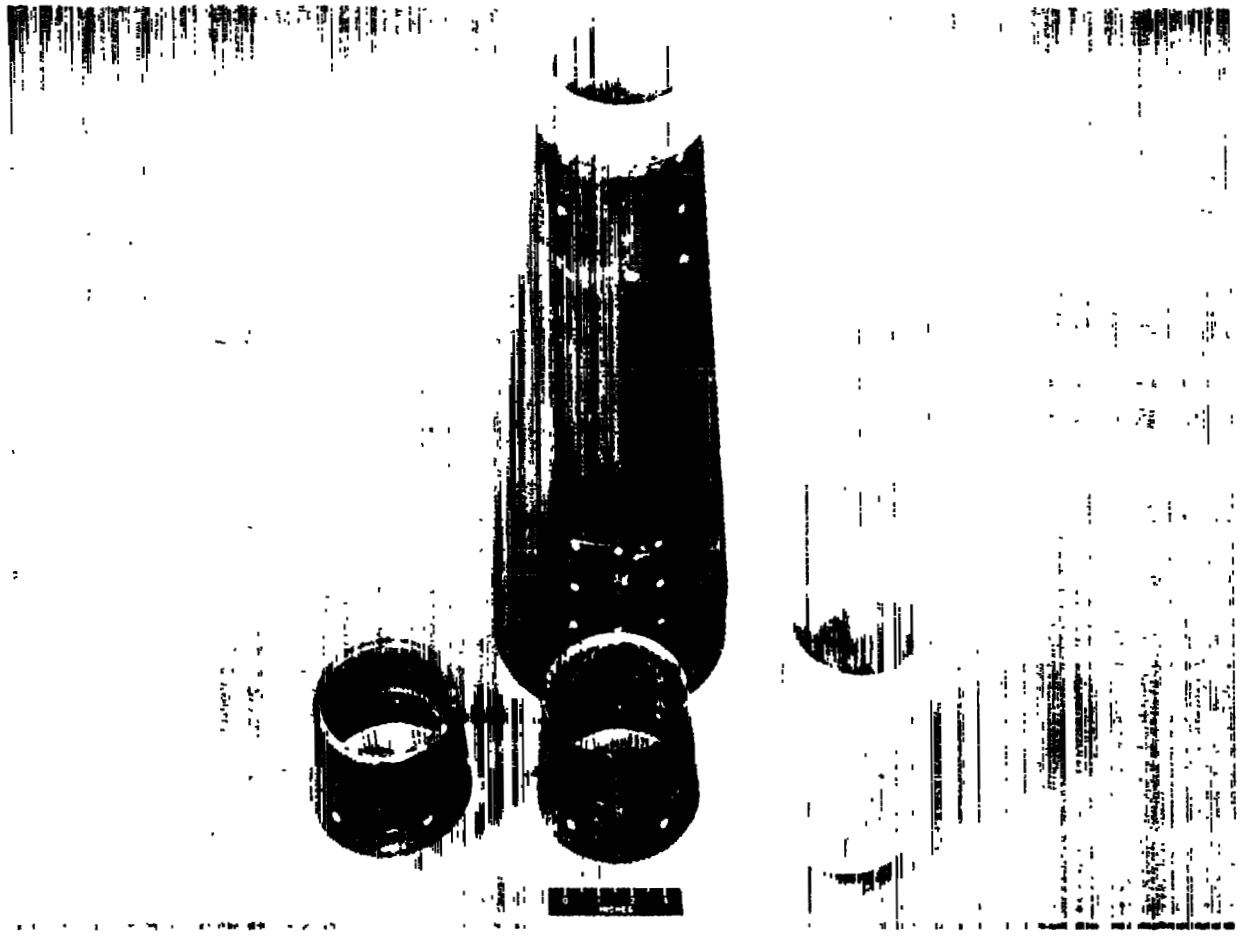

L-80764

(a) Three lip shapes and fixed portion.

Figure 3.- Conical-nose-inlet configurations. All dimensions are in inches.

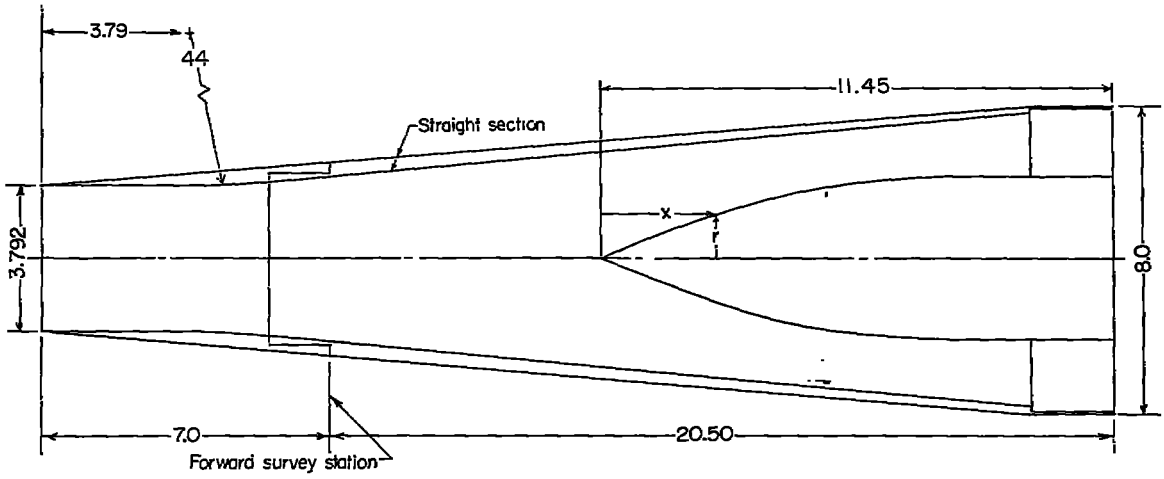

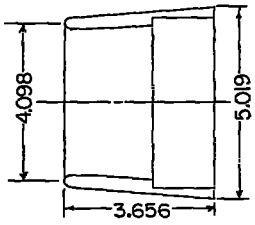

Central Fairing Coordinates

x, in.	r, in.
0	0
.625	.301
1.625	.736
2.625	1.113
3.625	1.432
4.625	1.693
5.625	1.895
6.625	2.040
7.625	2.127
8.625	2.156
12.45	2.156

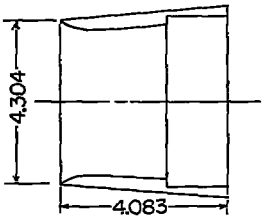

(b) General dimensions.

Figure 3.- Continued.

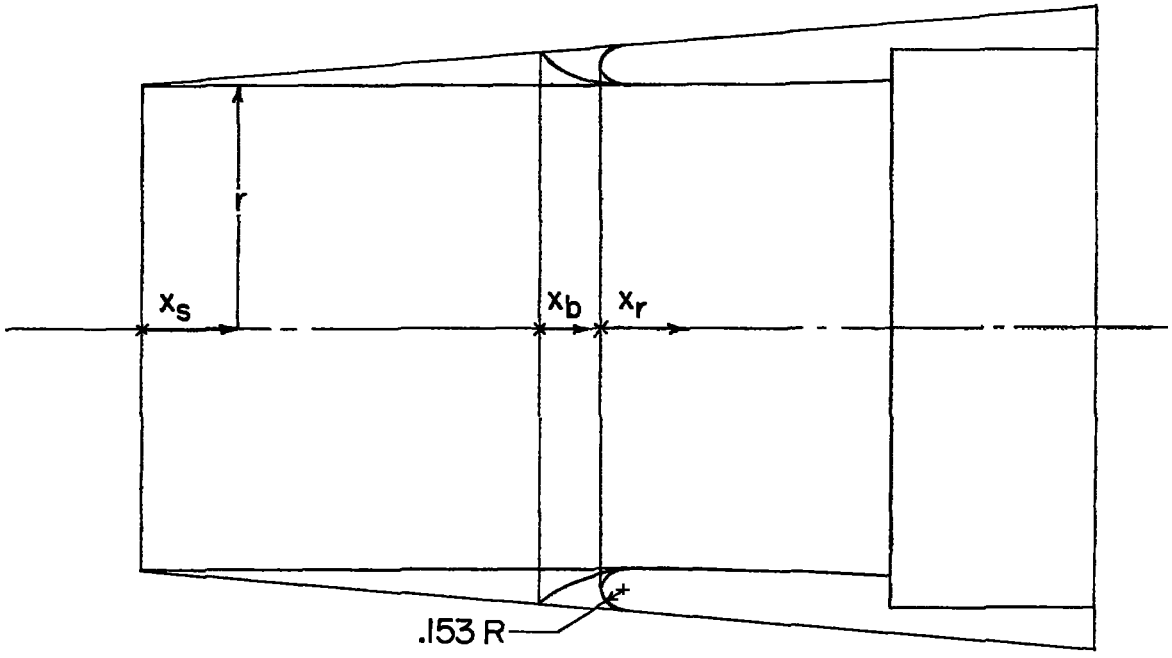

Inlet Inner-Lip Coordinates

Sharp lip		Bell lip		Round lip	
x_s, in.	r_s, in.	x_b, in.	r_b, in.	x_r, in.	r_r, in.
0	1.896	0	2.152	0	2.049
3.79	1.896	.04	2.117	.153	1.896
4.29	1.899	.08	2.086	.446	1.896
4.79	1.907	.18	2.018	.946	1.899
5.29	1.922	.28	1.964	1.446	1.907
5.79	1.942	.48	1.904	1.946	1.922
6.29	1.967	.873	1.896	2.446	1.942
6.79	1.998	1.373	1.899	2.946	1.967
7.29	2.035	1.873	1.907	3.446	1.998

A_{min} = 0.07845 sq ft

(c) Lip coordinates.

Figure 3.- Concluded.

[redacted]

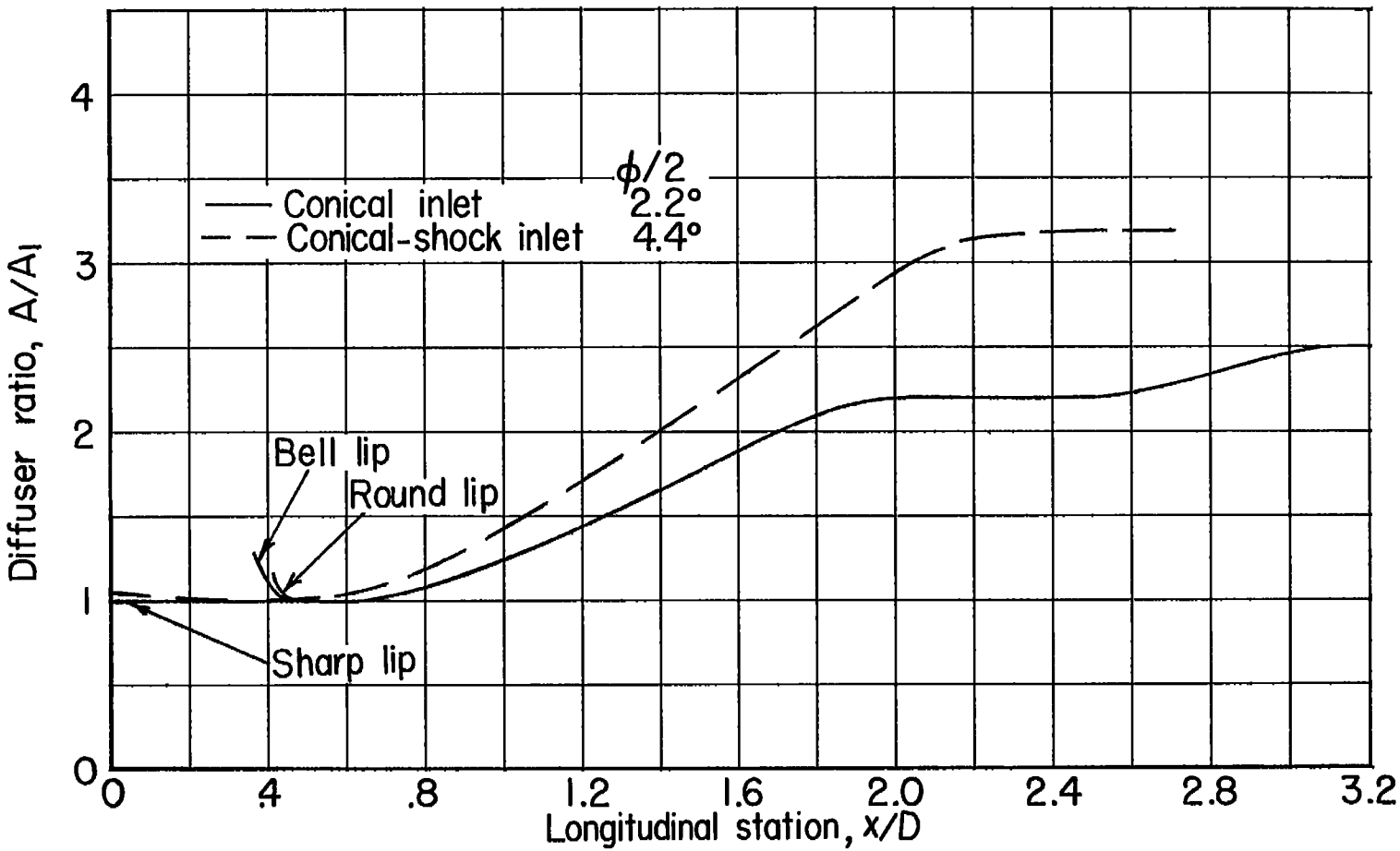

Figure 4.- Duct-area variation.

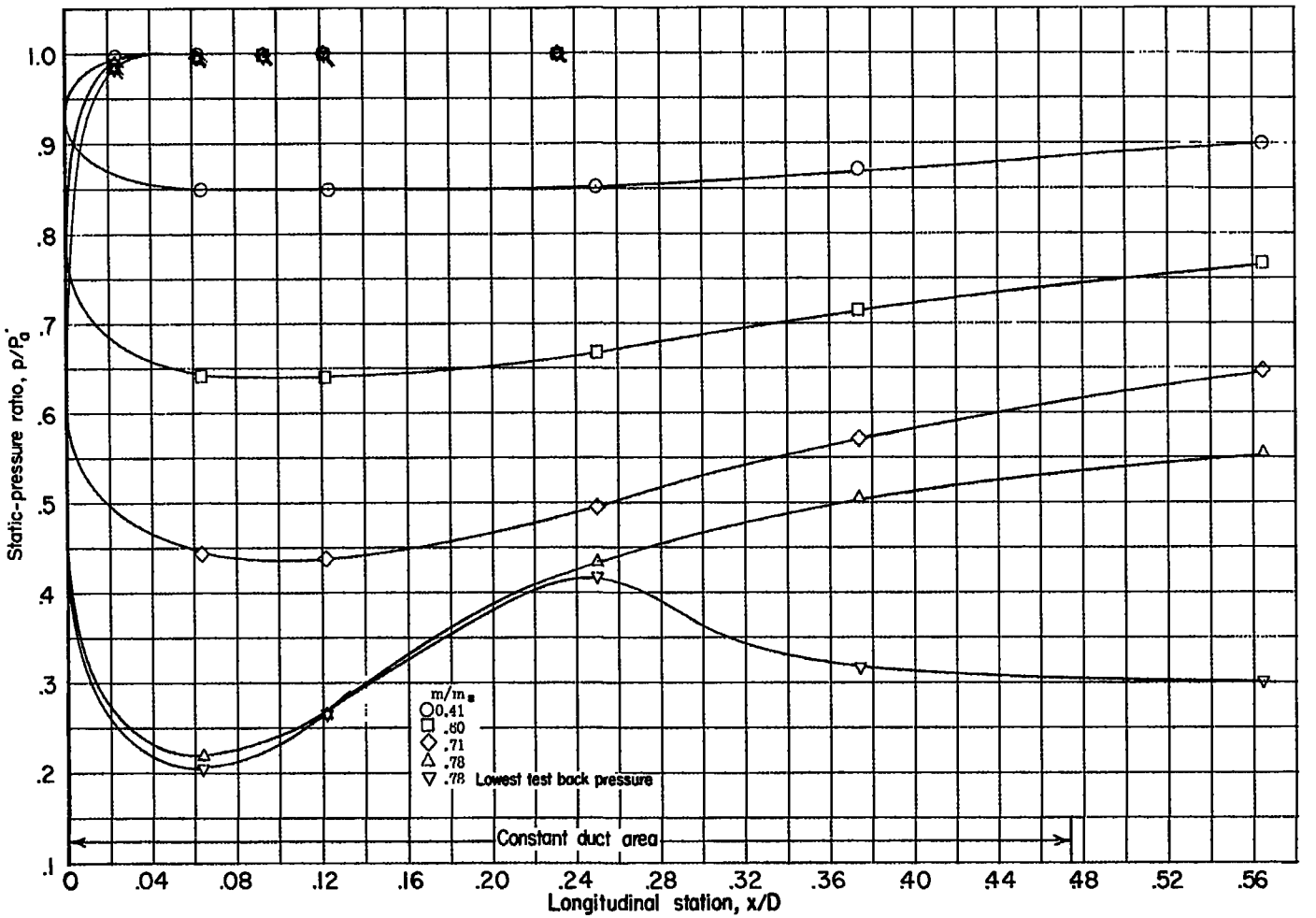

(a) Sharp lip.

Figure 5.- Inlet-lip pressure distributions. Flagged symbols denote outer surface pressures.

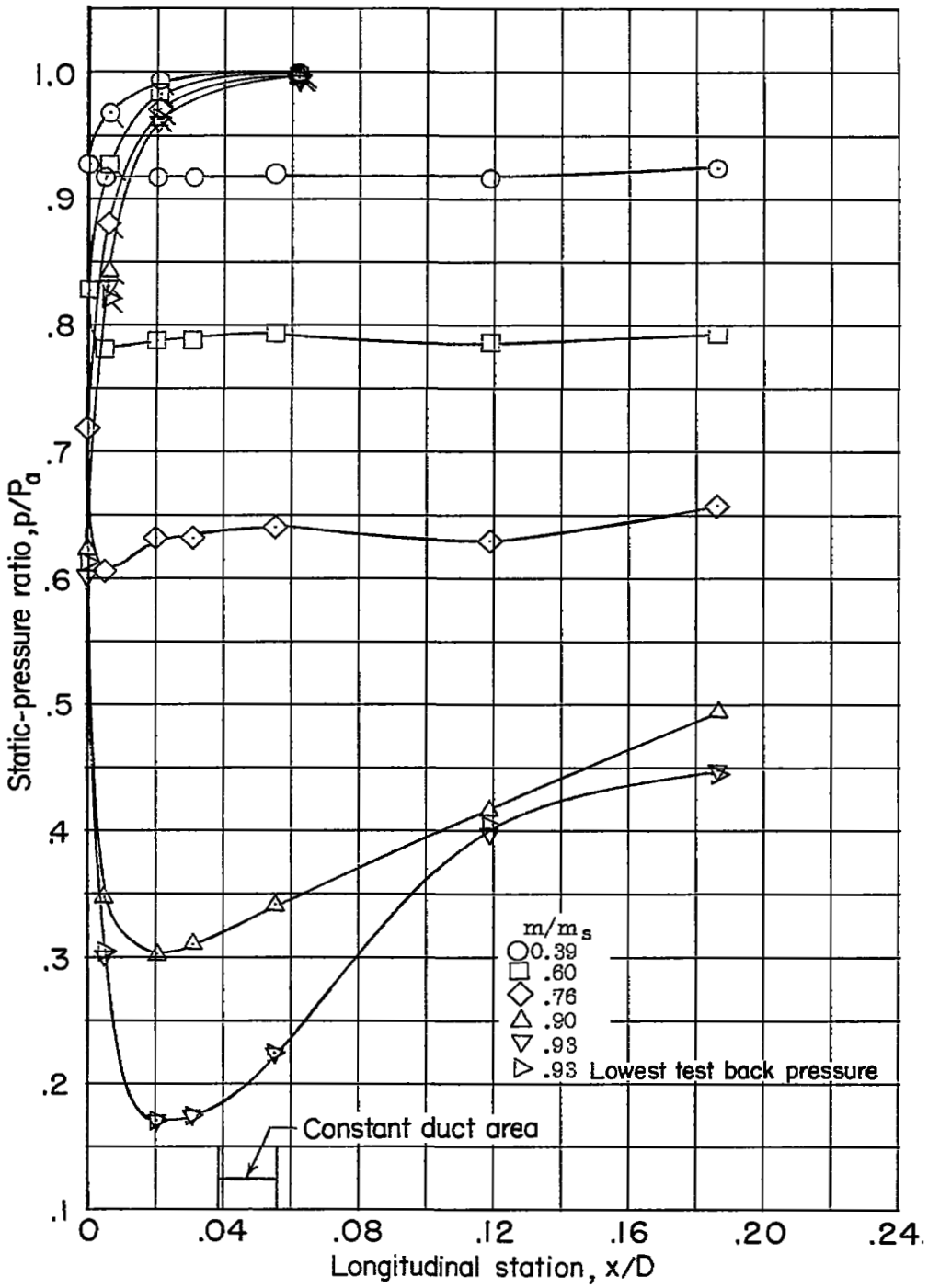

(b) Round lip.

Figure 5.- Continued.

[redacted]

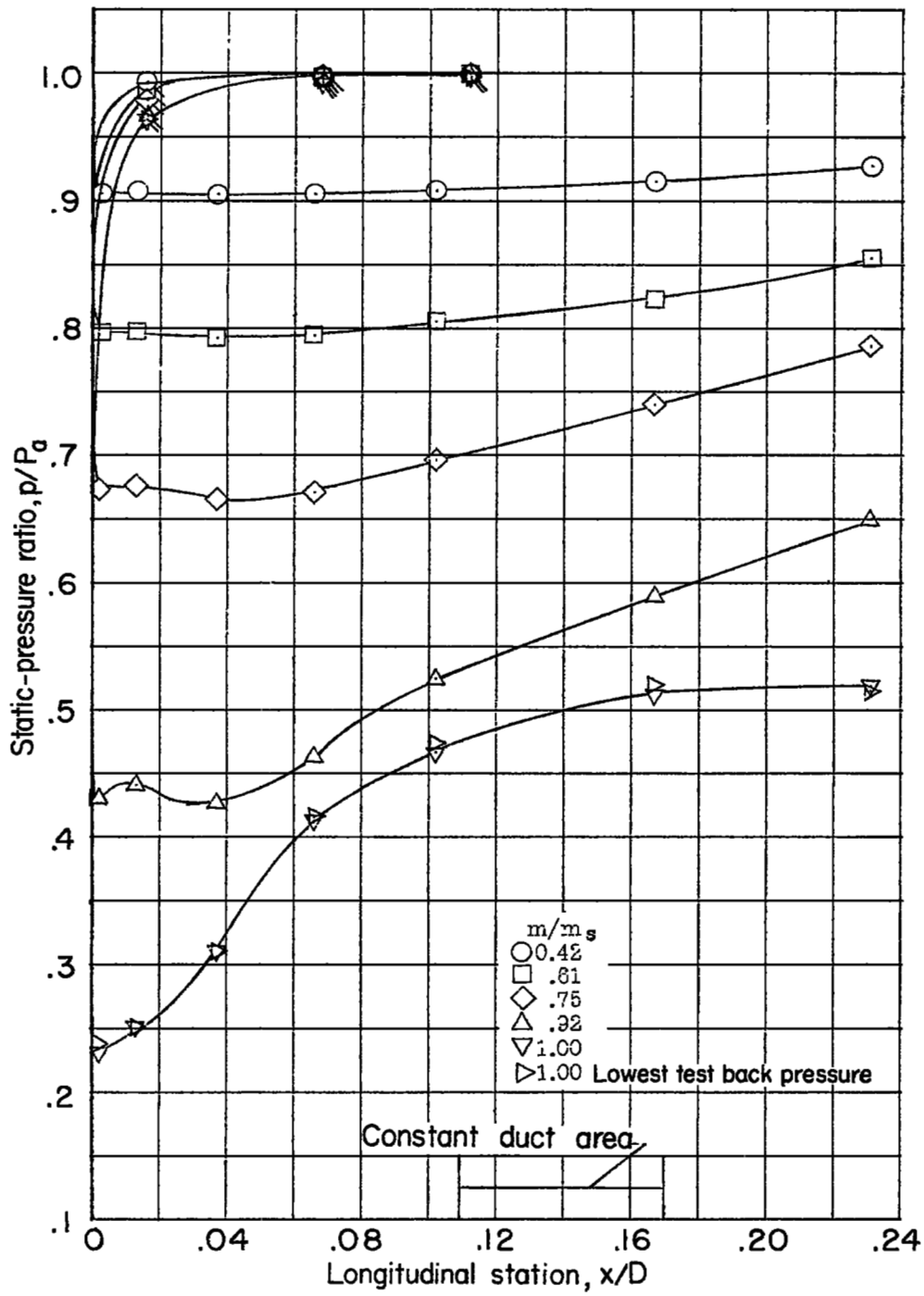

(c) Bell lip.

Figure 5.- Concluded.

[redacted]

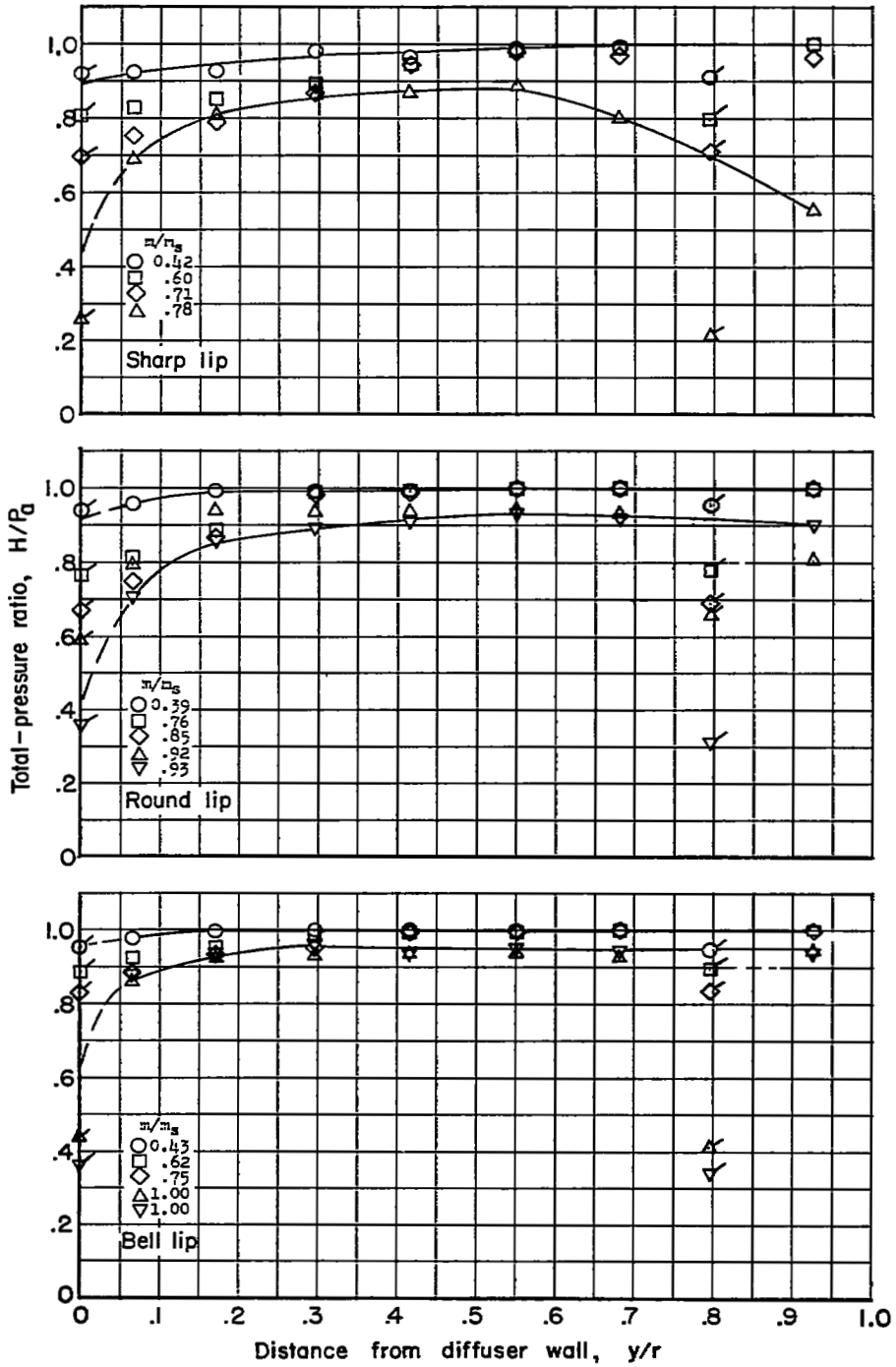

Figure 6.- Total-pressure profiles at forward survey station. Flagged symbols denote static-pressure ratio.

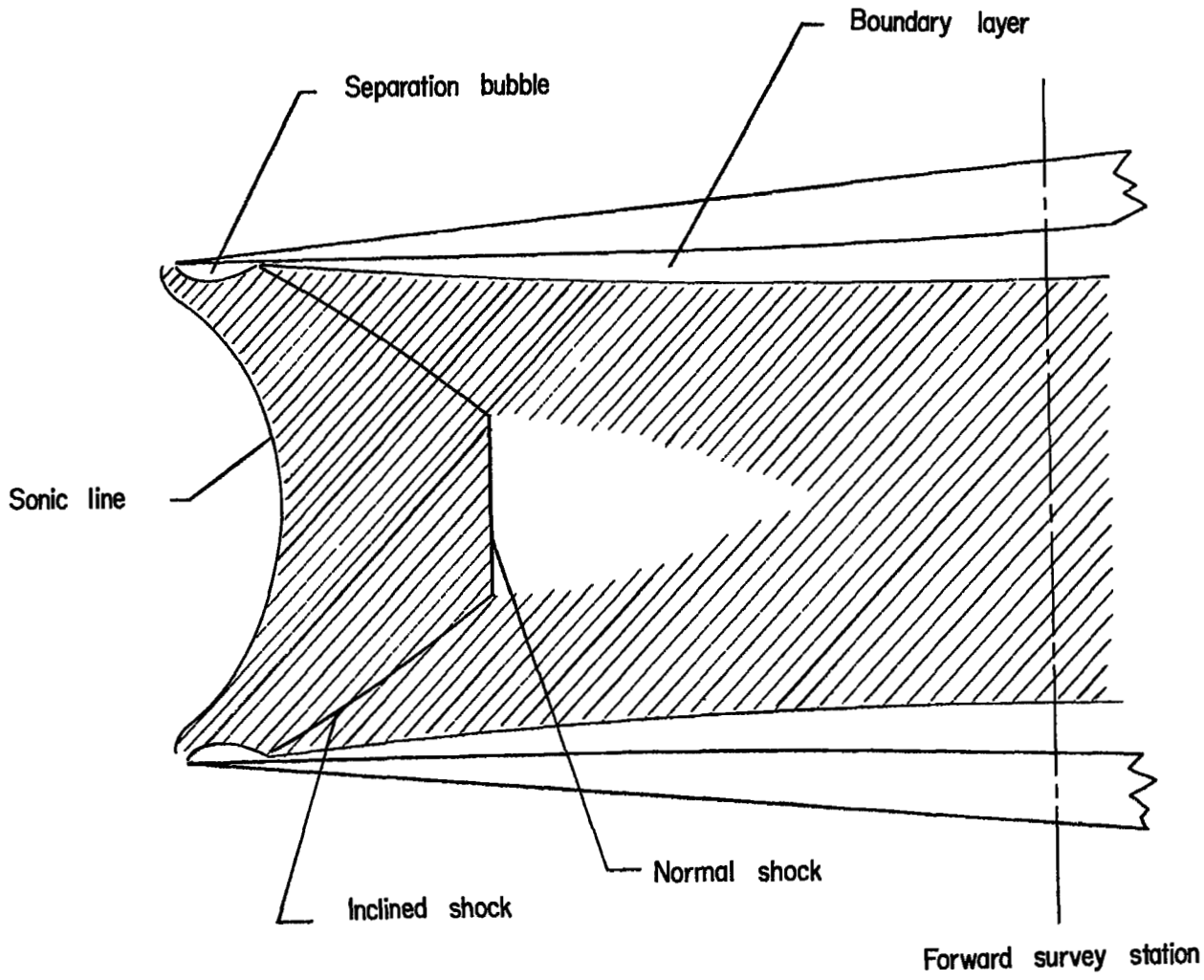

Figure 7.- Flow in sharp-lip inlet at choked condition. Regions of supersonic flow indicated by crosshatching.

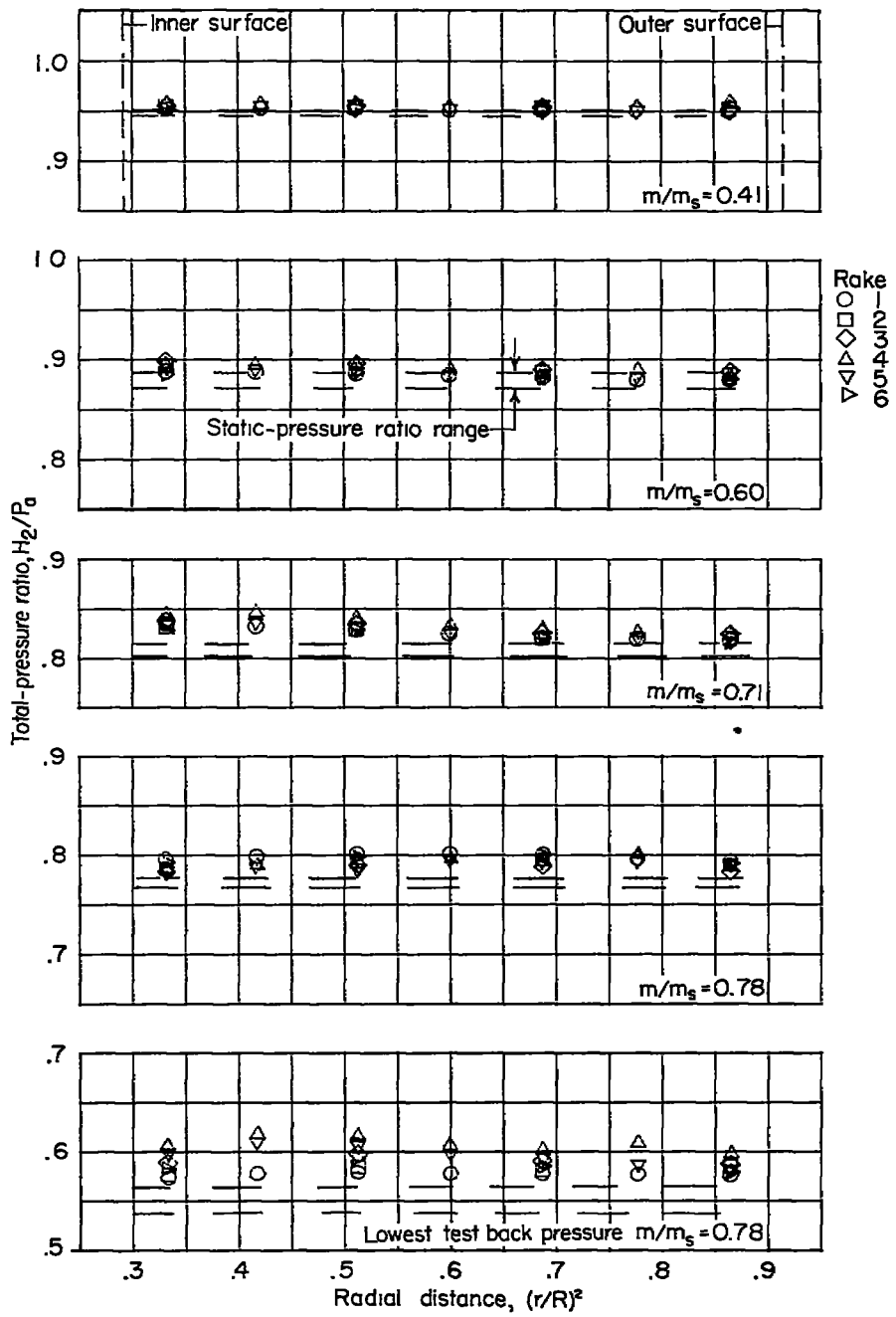

(a) Sharp lip.

Figure 8.- Variation of total-pressure ratio at station 2 with radial distance.

[redacted]

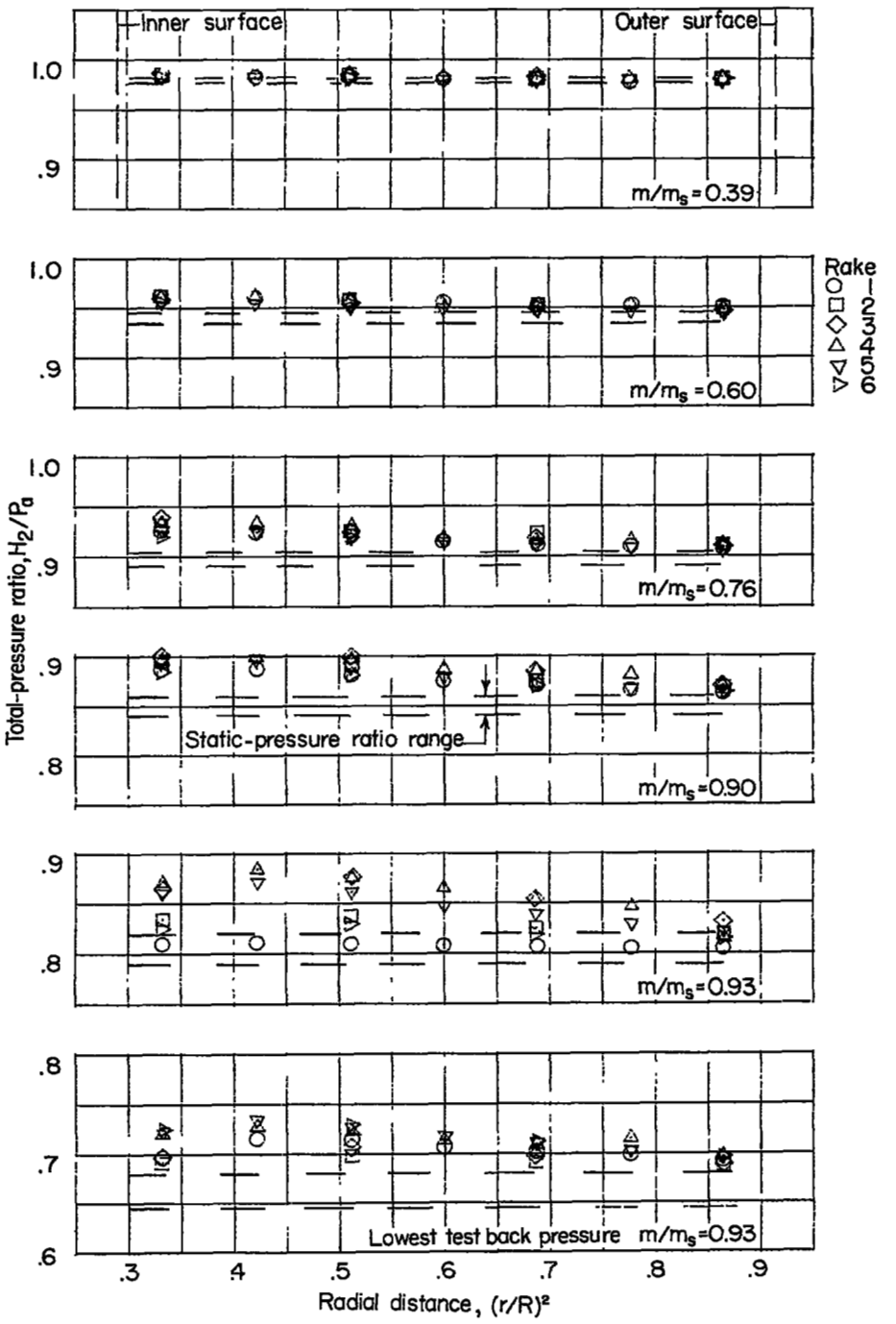

(b) Round lip.

Figure 8.- Continued.

[redacted]

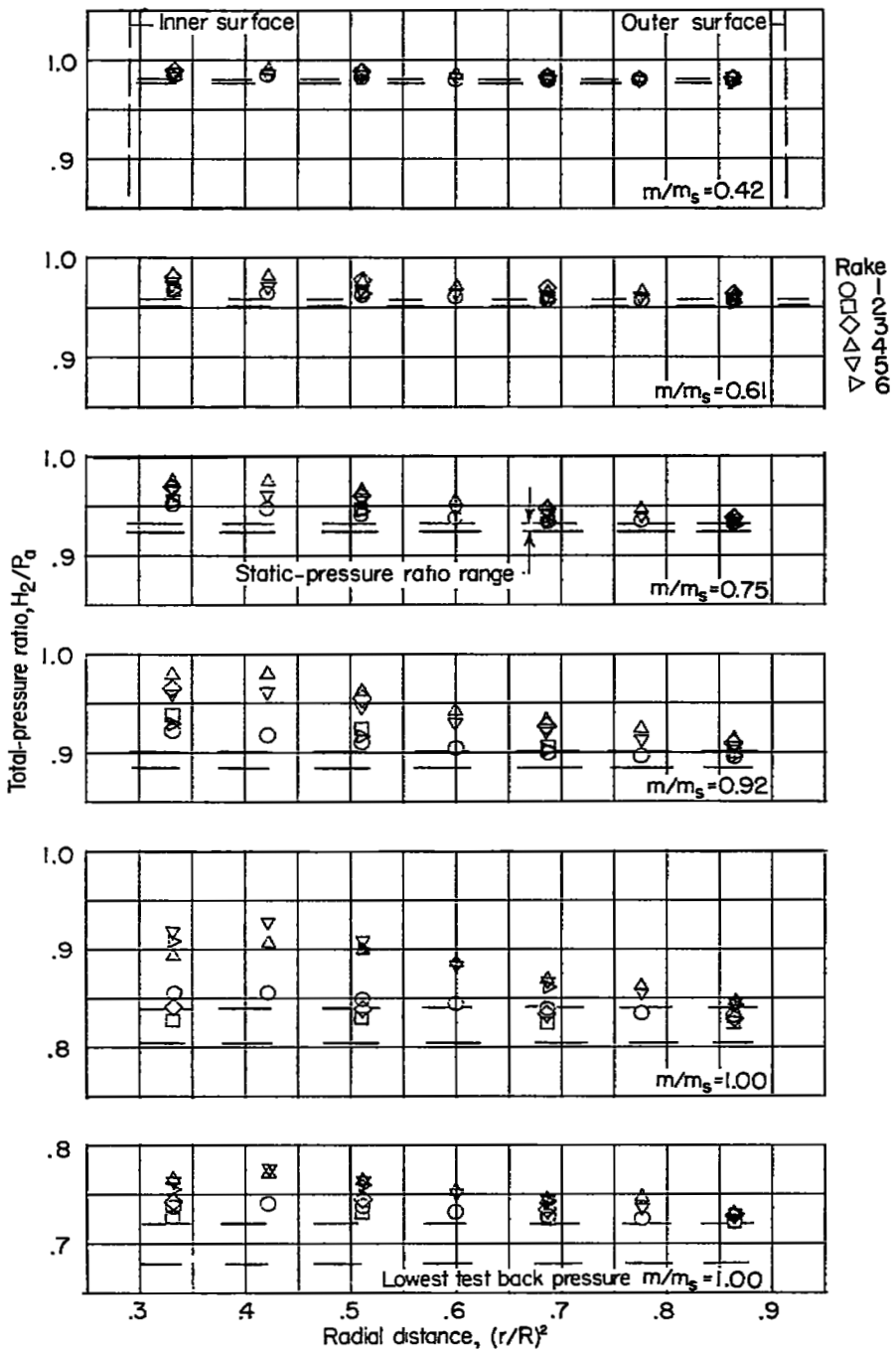

(c) Bell lip.

Figure 8.- Concluded.

[redacted]

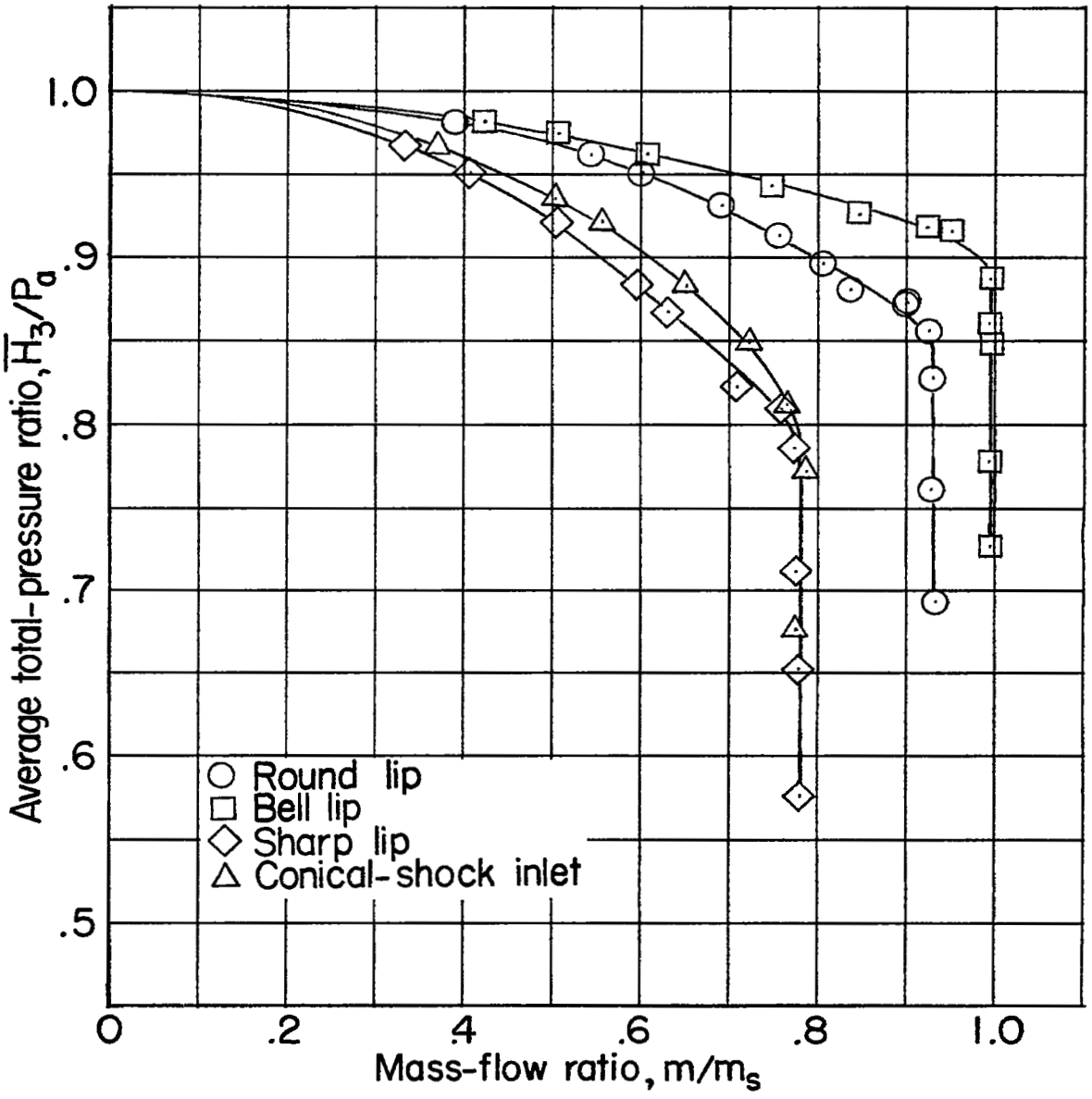

Figure 9.- Effect of mass flow on total-pressure ratio for inlets tested.

[redacted]

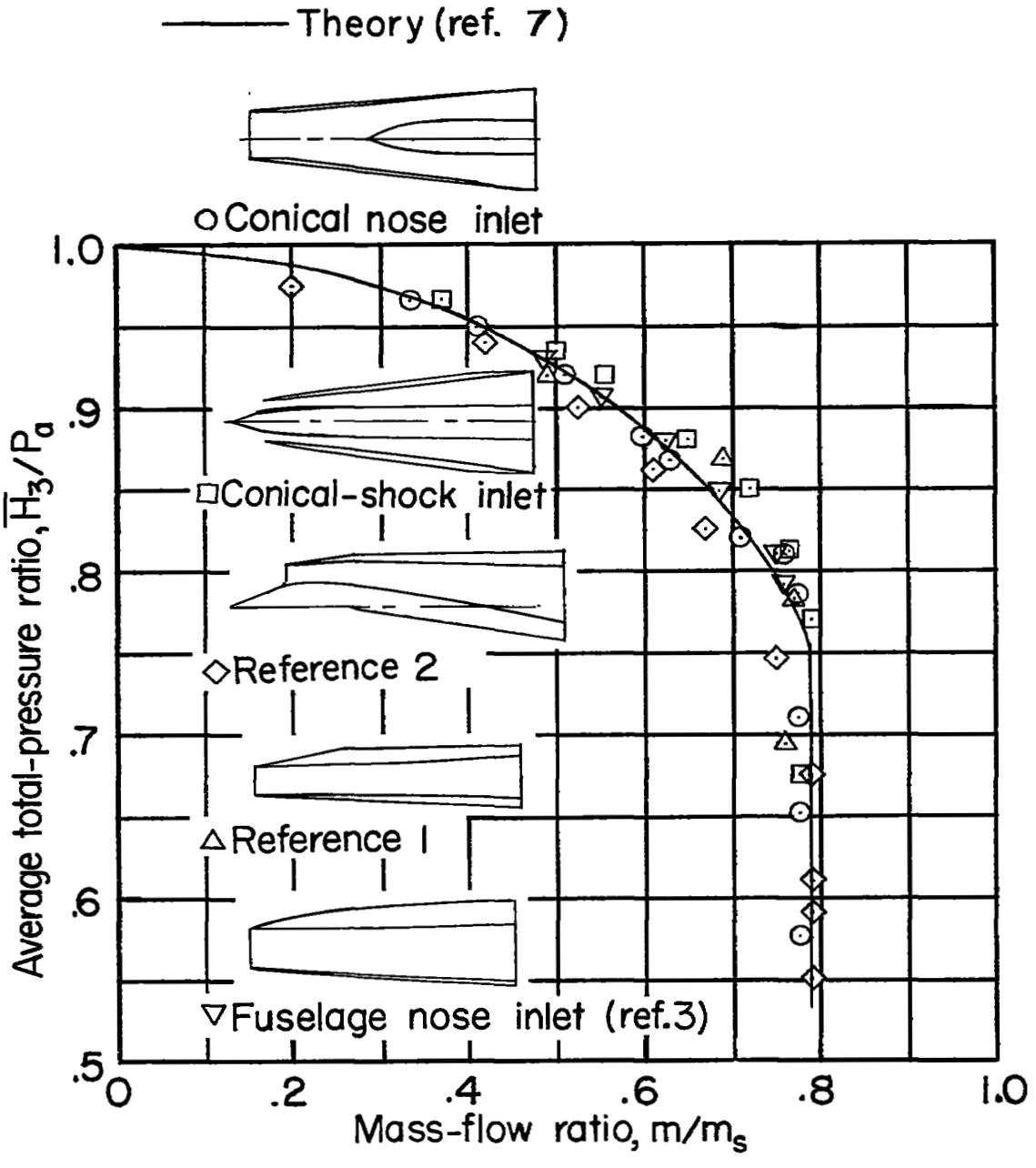

Figure 10.- Effect of mass-flow ratio on total-pressure ratio for thin sharp-lipped inlets.

NACA-Langley - 7-6-54 - 350